Brain Stimulation 11 (2018) 959–973

Contents lists available at ScienceDirect

Brain Stimulation

journal homepage: http://www.journals.elsevier.com/brain-stimulation

Whole-brain low-intensity pulsed ultrasound therapy markedly improves cognitive dysfunctions in mouse models of dementia - Crucial roles of endothelial nitric oxide synthase

Kumiko Eguchi [a], Tomohiko Shindo [a], Kenta Ito [a], Tsuyoshi Ogata [a], Ryo Kurosawa [a], Yuta Kagaya [a], Yuto Monma [a], Sadamitsu Ichijo [a], Sachie Kasukabe [a], Satoshi Miyata [a], Takeo Yoshikawa [b], Kazuhiko Yanai [b], Hirofumi Taki [c], Hiroshi Kanai [d], Noriko Osumi [e], Hiroaki Shimokawa [a, *]

[a] Department of Cardiovascular Medicine, Tohoku University Graduate School of Medicine, Sendai, Japan
[b] Department of Pharmacology, Tohoku University School of Medicine Sendai, Japan
[c] Biomedical Engineering for Health and Welfare, Graduate School of Biomedical Engineering, Tohoku University, Sendai, Japan
[d] Department of Electronic Engineering, Tohoku University Graduate School of Engineering, Sendai, Japan
[e] Department of Developmental Neuroscience, Tohoku University, Sendai, Japan

ARTICLE INFO

Article history:
Received 22 January 2018
Received in revised form
1 May 2018
Accepted 20 May 2018
Available online 22 May 2018

Keywords:
LIPUS
Dementia
eNOS

ABSTRACT

Background: Therapeutic focused-ultrasound to the hippocampus has been reported to exert neuroprotective effects on dementia. In the present study, we examined whether the whole-brain LIPUS (low-intensity pulsed ultrasound) therapy is effective and safe in 2 mouse models of dementia (vascular dementia, VaD and Alzheimer's disease, AD), and if so, to elucidate the common underlying mechanism(s) involved.

Methods: We used bilateral carotid artery stenosis (BCAS) model with micro-coils in male C57BL/6 mice as a VaD model and 5XFAD transgenic mice as an AD model. We applied the LIPUS therapy (1.875 MHz, 6.0 kHz, 32cycles) to the whole brain.

Results: In both models, the LIPUS therapy markedly ameliorated cognitive impairments (Y-maze test and/or passive avoidance test) associated with improved cerebral blood flow (CBF). Mechanistically, the LIPUS therapy significantly increased CD31-positive endothelial cells and Olig2-positive oligodendrocyte precursor cells (OPCs) in the VaD model, while it reduced Iba-1-positive microglias and amyloid-β (Aβ) plaque in the AD model. In both models, endothelium-related genes were significantly upregulated in RNA-sequencing, and expressions of endothelial nitric oxide synthase (eNOS) and neurotrophins were upregulated in Western blotting. Interestingly, the increases in glia cells and neurotrophin expressions showed significant correlations with eNOS expression. Importantly, these beneficial effects of LIPUS were absent in eNOS-knockout mice.

Conclusions: These results indicate that the whole-brain LIPUS is an effective and non-invasive therapy for dementia by activating specific cells corresponding to each pathology, for which eNOS activation plays an important role as a common mechanism.

1. Introduction

Novel, effective strategies for treating dementia are urgently needed, particularly given alarming increases in the global prevalence of dementia. According to the current estimates, nearly 47 million patients worldwide had dementia in 2015, and this number is estimated to exceed 131 million by 2050 [1]. However, no curative treatment is yet available for vascular dementia (VaD) or Alzheimer's disease (AD) [2,3], both of which comprise the most common causes of dementia. VaD and AD share risk factors, such as hypertension, hypercholesterolemia, and diabetes mellitus [2,3]. Long-term exposure to these risk factors results in common outcome, i.e., impairment of vascular endothelial functions [4].

* Corresponding author. Department of Cardiovascular Medicine, Tohoku University Graduate School of Medicine, 1-1 Seiryo-machi, Aoba-ku, Sendai, 980-8574, Japan.
E-mail address: shimo@cardio.med.tohoku.ac.jp (H. Shimokawa).

https://doi.org/10.1016/j.brs.2018.05.012

Abbreviations

Aβ	amyloid-beta
AD	Alzheimer's disease
APP	amyloid precursor protein
BACE-1	β-site APP-cleaving enzyme-1
BCAS	bilateral carotid artery stenosis
BDNF	brain-derived neurotrophic factor
CBF	cerebral blood flow
CREB	cAMP response element-binding protein
CXCR4	CXC chemokine receptor 4
DCX	doublecortin
eNOS	endothelial nitric oxide synthase
FGF-2	fibroblast growth factor-2
GFAP	glial fibrillary acidic protein
GO	gene ontology
Iba-1	ionized calcium-binding adapter molecule-1
iNOS	inducible nitric oxide synthase
LIPUS	low-intensity pulsed ultrasound
MAPK	mitogen-activated protein kinase
NGF	nerve growth factor
nNOS	neuronal nitric oxide synthase
OPC	oligodendrocyte precursor cell
Hsp 90	heat shock protein 90
RNA-seq	RNA-sequencing
VaD	vascular dementia
VEGF	vascular endothelial growth factor
WML	white matter lesions

Thus, the endothelium has been recognized as an important and common therapeutic target for prevention and treatment of dementia [4].

Among several reports on therapeutic applications of ultrasound technology, low-intensity pulsed ultrasound (LIPUS) has emerged as a non-invasive therapy for several diseases. We have previously demonstrated that vascular endothelial cells substantially contribute to the therapeutic effect of LIPUS, inducing therapeutic angiogenesis in myocardial ischemia [5,6]. Meanwhile, LIPUS has also been reported to increase the production of brain-derived neurotrophic factor (BDNF) in astrocytes [7] and nerve growth factor (NGF) in PC12 cells [8], and to promote nerve regeneration [9]. Also, focused LIPUS to the hippocampus could ameliorate dementia (VaD and AD) in mice via increasing endogenous neurotrophins and vascular endothelial growth factor (VEGF) [10,11]. However, it is still unknown what kind of cell type contributes to the LIPUS-induced cognitive improvement, and whether there is a common factor in the two disorders. Moreover, from clinical point of view, we hypothesized that whole-brain LIPUS, rather than focused ultrasound, is effective and feasible since VaD is characterized by the widespread white matter lesions (WML) and AD by the widespread deposition of amyloid-β (Aβ) in the brain [2,3]. Thus, in the present study, we aimed to examine the effectiveness and safety of whole-brain LIPUS therapy that has never been used before. We first examined whether the whole-brain LIPUS is effective in different mouse models of dementia (VaD and AD), and if so, to elucidate the common mechanism underlying the beneficial effects of LIPUS.

2. Methods

See Supplementary Methods.

3. Results

3.1. LIPUS therapy improves cognitive dysfunctions in the VaD model

In the VaD model, the LIPUS therapy (Fig. 1A and B, Supplementary Figs. 1A and B) had no effects on body weight or systolic blood pressure (Supplementary Fig. 1C). LIPUS-treated mice showed no signs of cramps, paralysis, cerebral hemorrhage, hypothermia, hyperthermia, or increased mortality compared with control mice, which underwent the same procedure without LIPUS treatment (data not shown). In the Y-maze test, the number of entries was comparable between the LIPUS and control groups, suggesting that LIPUS causes no hyperactivity (Fig. 1C). Next, the LIPUS-treated BCAS group had significantly improved performance for cognitive functions, including spontaneous alternation task in the Y-maze and retention in the passive avoidance test (Fig. 1C). In the novel object recognition test, the LIPUS-treated BCAS group tended to have improved cognitive function compared with the control group (Fig. 1C). Similar results were also obtained at 56 and 84 days after the LIPUS therapy (Supplementary Fig. 1D), and there were no side effects of LIPUS for 3 months (data not shown). The LIPUS therapy significantly improved cerebral blood flow (CBF) in the BCAS group for up to 28 days after the therapy, whereas it had no effect in the control groups (Fig. 1D). Taken together, these results suggest that the cognitive improvement by the LIPUS therapy is associated with increased CBF and can last for at least 3 months.

3.2. LIPUS therapy improves WML in the VaD model

Next, we examined brain histology to determine the mechanism of the beneficial effects of the LIPUS therapy in the VaD model. We focused on the constituent cells of neurovascular unit possibly contributing to multifaceted actions of LIPUS. The results showed that the number of cells in the corpus callosum that were positive for GST-π, a marker of mature oligodendrocytes, was significantly higher in the LIPUS-treated group compared with the control group (Fig. 2A). In addition, Klüver-Barrera staining showed that the LIPUS therapy reduced the severity of WML following BCAS (Fig. 2A). Although there was no difference in CD31-positive cells in the corpus callosum (for assessment of capillary density), significantly more CD31-positive cells were present in the hippocampus of LIPUS-treated group compared with control group (Fig. 2A). Compared with control group, LIPUS-treated group showed no difference in the number of cells positive for GFAP (glial fibrillary acidic protein; for astrocytes) or Iba-1 (ionized calcium-binding adapter molecule-1; for microglias) (Supplementary Fig. 2). Moreover, doublecortin (DCX) staining of the hippocampus showed significantly more newly formed neurons in the dentate gyrus of LIPUS-treated group compared with control group (Fig. 2B, Supplementary Fig. 3). These results suggest that the LIPUS-induced angiogenesis ameliorates cognitive dysfunctions through neurogenesis and reduction of WML. Since we found no significant difference between the LIPUS-treated sham group and the control group, we focused on the BCAS group in the subsequent biochemical analyses.

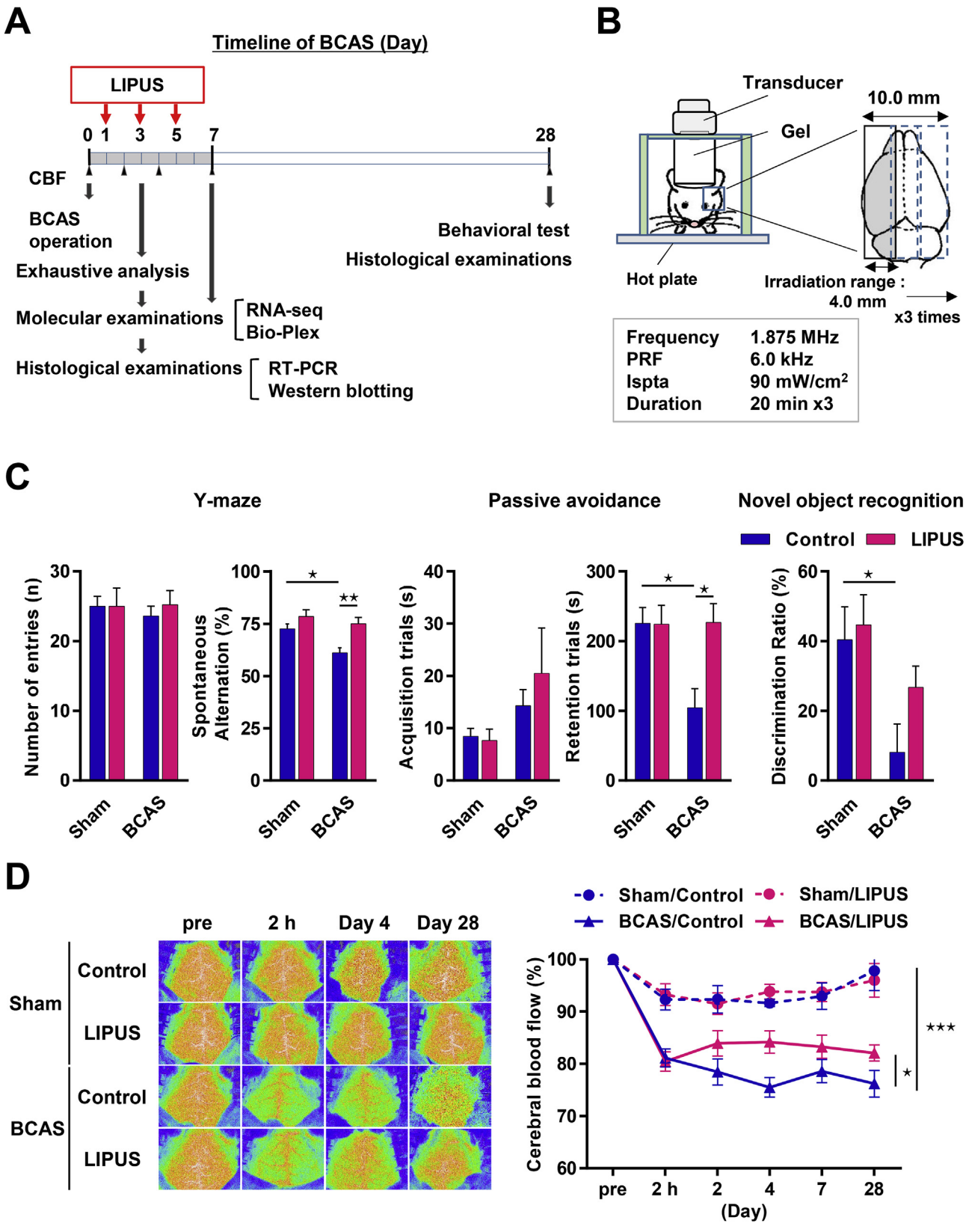

Fig. 1. Whole-brain LIPUS therapy improves cognitive dysfunctions in the VaD model.
(A) The timeline of the BCAS experiments. **(B)** Schematic drawing showing the application of whole-brain LIPUS in mice. **(C)** Behavioral testing was performed on day 28 following BCAS or sham surgery; n = 12–17 (Y-maze and Passive avoidance) and n = 5–12 (Novel object recognition).
(D) Representative images of cerebral blood flow (CBF) measured using laser speckle and time-course of CBF relative to baseline; n = 9–10 (sham) and n = 20–25 (BCAS). $^{*}P<0.05$, $^{**}P<0.005$, and $^{***}P<0.0005$ (two-way ANOVA). LIPUS, low-intensity pulsed ultrasound.
Sham/Control; sham operation without the LIPUS treatment.
Sham/LIPUS; sham operation with the LIPUS treatment.
BCAS/Control; BCAS operation without the LIPUS treatment.
BCAS/LIPUS; BCAS operation with the LIPUS treatment.

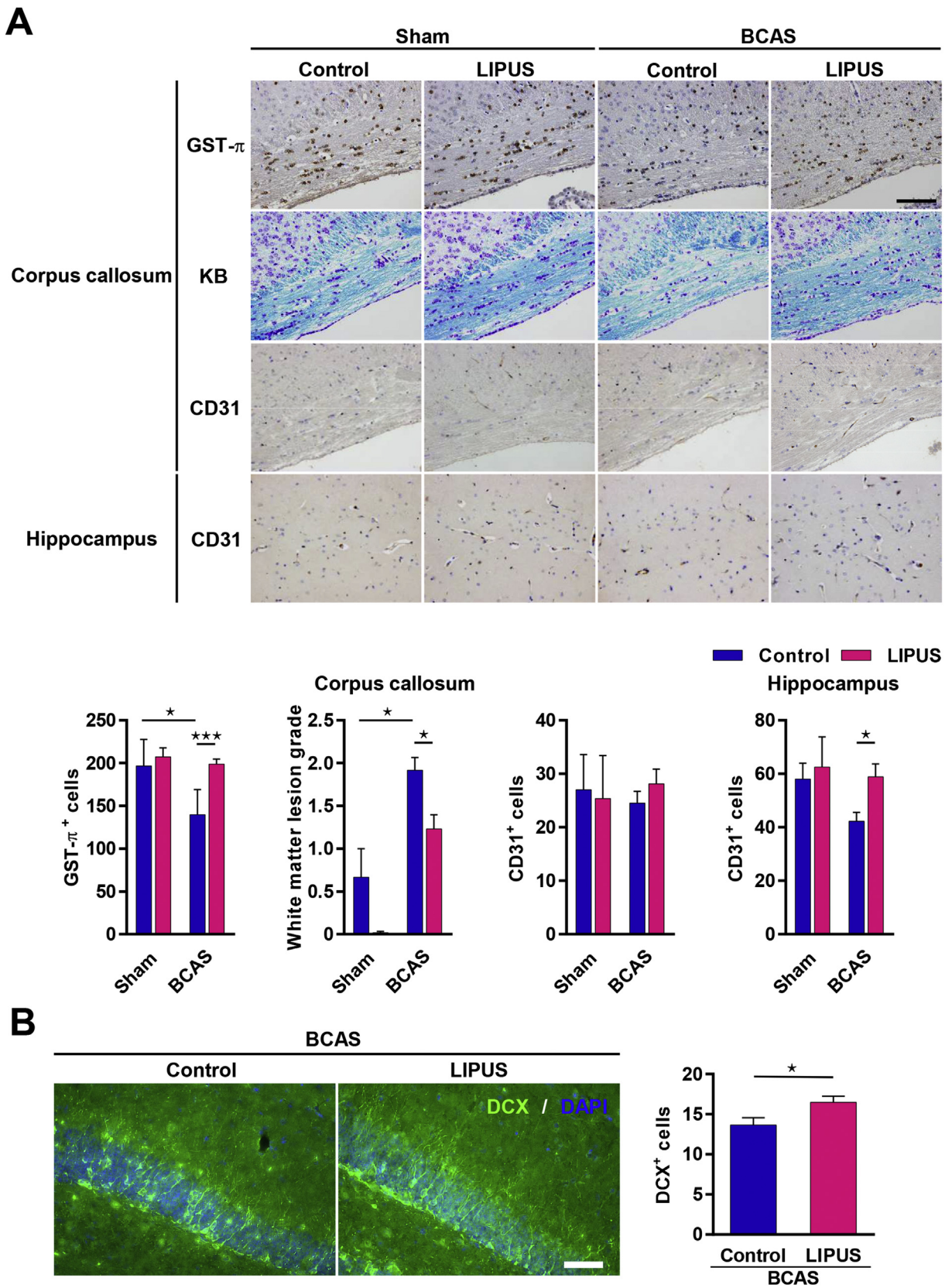

Fig. 2. LIPUS therapy enhances angiogenesis and reduces the severity of WML in the VaD model.
(A) Representative images of corpus callosum and hippocampal sections stained for GST-π, Klüver-Barrera (KB), and CD31 on day 28 following sham surgery or BCAS. The scale bar represents 100 μm. Quantitative analysis of GST-π-positive cells, white matter lesion severity, and CD31-positive cells in the corpus callosum and hippocampus; n = 3 (sham) and n = 12–13 (BCAS). **(B)** Representative images of hippocampal sections stained for DCX on day 28. The scale bar represents 50 μm. Quantitative analysis of DCX-positive cells in the hippocampus (n = 12–13). $^{*}P<0.05$ and $^{***}P<0.0005$ (**A**; two-way ANOVA, **B**; Student's *t*-test).

3.3. LIPUS therapy upregulates genes related to OPC and angiogenesis in the VaD model

To examine the effects of the LIPUS therapy at the molecular level, we performed RNA-sequencing (RNA-seq) using total brain samples. The results showed that 3 days after BCAS, the expressions of ~2000 genes differed significantly between the LIPUS-treated and control groups; specifically, 981 and 1239 genes were significantly upregulated and downregulated, respectively (Fig. 3A). Gene ontology (GO) term analysis showed that the genes differentially regulated by the LIPUS therapy were enriched for genes that play a role in angiogenesis and proliferation (Fig. 3B). Regarding the cell type responding to the LIPUS therapy, the highest number of LIPUS-enhanced genes was annotated to astrocytes, followed by genes annotated to endothelial cells and oligodendrocytes (Fig. 3C). Most of the genes listed as oligodendrocyte-related genes were annotated as playing a role in cell differentiation and development; however, since mature oligodendrocytes do not proliferate, these oligodendrocyte-related genes were likely to be oligodendrocyte precursor cells (OPCs). A heat map of upregulated and downregulated genes confirmed that the differentially expressed genes in response to LIPUS were related to astrocytes, OPCs, myelination, and angiogenesis (Fig. 3D).

To confirm our RNA-seq data, we performed RT-qPCR analyses for the following genes; GFAP (for astrocytes), Olig2 (for OPCs), eNOS (for angiogenesis and vasodilatation), and FGF-2 (fibroblast growth factor-2) and CXCR4 (CXC chemokine receptor 4) (for angiogenesis [12,13] and OPC differentiation [14,15]). mRNA levels of all 5 genes were higher in the LIPUS group compared with the control group (Fig. 3E).

In contrast, regarding the trend for improved histological and CBF state in the sham-operation group in response to LIPUS, we assumed the following hypothesis; since the sham-operation/LIPUS group underwent the same procedure with BCAS except the placement of micro-coils, those mice were under temporary ischemic burden. In fact, CBF in the sham-operated groups decreased to ~90% compared with baseline CBF at 2 h to 7 days after operation. We do not consider that this mild decrease in CBF led to cerebral dysfunction including cognitive function. We rather hypothesize that LIPUS treatment has a potential to upregulate angiogenesis-related genes. To confirm this hypothesis, we performed RNA-seq analysis with sham group animals and found that LIPUS upregulated angiogenesis-related genes including eNOS (Supplementary Fig. 4).

3.4. LIPUS increases the protein levels related to angiogenesis, OPC-genesis, and neurotrophins in the VaD model

Next, we examined the effect of the LIPUS therapy at the protein level. The results of multiplex analysis using Bio-Plex showed that LIPUS increased proteins in the MAPK (mitogen-activated protein kinase) pathway, including CREB (cAMP response element-binding protein), ERK1/2, MEK, p38 MAPK, and proteins downstream of the PI3K/Akt pathway, including p70 S6 kinase, whereas GSK-3αβ was slightly but significantly decreased (Supplementary Fig. 5A). To confirm this finding, we measured the extent of phosphorylation of ERK1/2 and Akt, which are main mediators of the MAPK and PI3K-Akt pathways for angiogenesis and cell proliferation, respectively. We found that p-ERK1/2 was significantly increased in the LIPUS-treated group on day 3, but not on day 7 (Supplementary Fig. 5B). In contrast, p-Akt did not differ between the LIPUS-treated and control groups at either time point (Supplementary Fig. 5B).

We thus measured the protein levels of GFAP, Olig2, eNOS, CXCR4, and FGF2 as mRNA expressions of those factors were increased by LIPUS, and nerve growth factor (NGF), pro-BDNF, and VEGF (vascular endothelial growth factor) as those were reported to be increased by LIPUS [7,8]. As shown in Fig. 3F and Supplementary Fig. 5D, the protein levels of GFAP, p-eNOS, t-eNOS, FGF2, NGF, and pro-BDNF were significantly higher in the LIPUS group on day 3, whereas those of Olig2, CXCR4, and VEGF were unchanged at this time point. In contrast, t-eNOS, CXCR4, FGF2, VEGF, and NGF, but not GFAP, Olig2, p-eNOS or pro-BDNF, were significantly increased in the LIPUS group on day 7 (Supplementary Figs. 5C and 5D). Interestingly, we found a positive correlation between eNOS expression and NGF, pro-BDNF, and VEGF (Fig. 3G), indicating that the expression of neurotrophins is correlated with eNOS expression. Besides, LIPUS had no significant effect on neuronal NO synthase (nNOS) or inducible NO synthase (iNOS) at either time point (Supplementary Fig. 6A). Thus, the upregulation of endogenous growth factors in the LIPUS-treated group may contribute to improved cognitive functions, for which eNOS plays an important role.

3.5. LIPUS enhances OPC proliferation in the VaD model

Mechanistically, we examined histological changes in the corpus callosum and hippocampus on day 3 after BCAS surgery. In the corpus callosum, the LIPUS therapy significantly increased the number of Olig2-positive cells in the BCAS group, but had no significant effect on GFAP-positive or Ki67-positive cells (Fig. 4A). In contrast, in the hippocampus, LIPUS significantly increased the number of Ki67-positive cells in the BCAS group, but had no significant effect on GFAP-positive or Olig2-positive cells (Fig. 4A). We also examined which cell types are involved in LIPUS-induced proliferation by co-immunostaining for Ki67 and Olig2, and found that the LIPUS therapy increases OPC proliferation (Fig. 4B). In contrast, by staining both eNOS and CD31, we found that eNOS was expressed specifically in the vascular endothelium of the corpus callosum following the LIPUS therapy (Supplementary Fig. 6B). Furthermore, consistent with our Western blot analysis, immunostaining showed that eNOS expression was increased following the LIPUS therapy in the BCAS group (Supplementary Fig. 6C). We also found a positive correlation between eNOS and Olig2 and between eNOS and GFAP (Fig. 4C). Taken together, these results suggest that the whole-brain LIPUS therapy in mice with BCAS activated OPCs and astrocytes associated with eNOS upregulation.

3.6. Essential role of eNOS in the beneficial effects of the LIPUS therapy in the VaD model

We next examined the role of eNOS in the LIPUS-induced improvement in cognitive function using eNOS-knockout ($eNOS^{-/-}$) mice. The LIPUS therapy had no significant effect on BCAS-induced changes in CBF (Fig. 5A). Importantly, in $eNOS^{-/-}$ mice, LIPUS had no beneficial effects on BCAS-induced behavior outcome (Fig. 5B), the number of GST-π-positive cells, the extent of WML, or the number of CD31-positive cells (Fig. 5C). Moreover, the expression levels of VEGF and neurotrophins, both of which were significantly increased in LIPUS-treated wild-type mice with BCAS, were unaffected by the LIPUS therapy in $eNOS^{-/-}$ mice (Fig. 5D). Thus, we conclude that eNOS is crucial for mediating the beneficial effects of the LIPUS therapy in the VaD model.

3.7. LIPUS therapy ameliorates cognitive dysfunctions in the AD model

Next, we examined the effect of another common form of dementia, Alzheimer's disease (AD), using 5XFAD mice (Fig. 6A), an established mouse model of AD pathology [16]. We first confirmed that whole-brain LIPUS had no effects on body weight or systolic

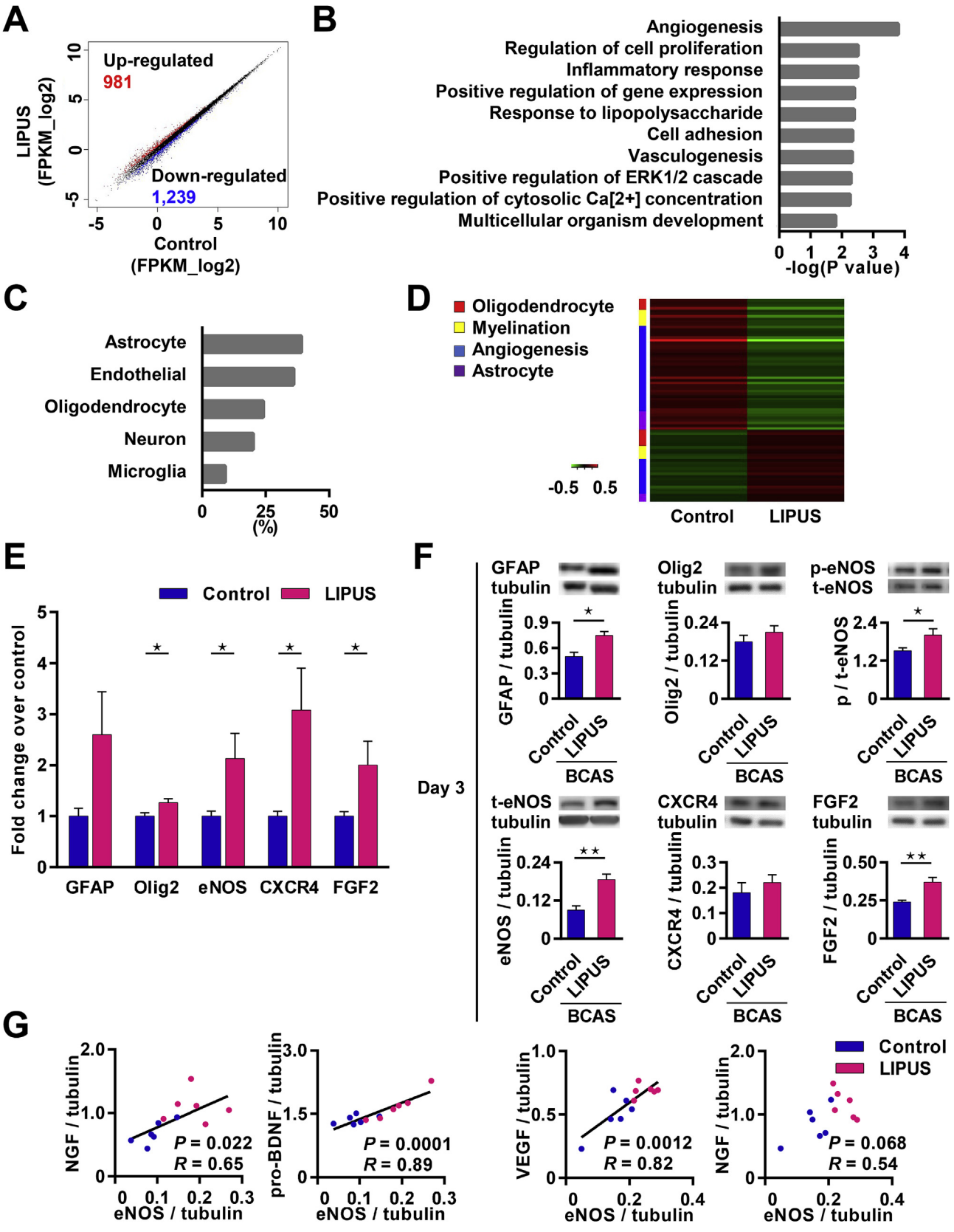

Fig. 3. LIPUS therapy enhances angio-, OPC-genesis-related molecules, and neurotophins in correlation with eNOS.
(A) Scatter plot depicting differential gene expression between the LIPUS-treated BCAS group and the control BCAS group on day 3. Significantly upregulated or downregulated genes are colored in red and blue, respectively. **(B)** Gene ontology (GO) analyses of the significantly upregulated and downregulated genes between the LIPUS-treated and control BCAS groups. The top 10 GO terms are shown in descending order of *P*-value. **(C)** The percentage of differentially regulated genes for each cell type annotated by GO terms. **(D)** Heat map depicting the relative expressions of the genes related to angiogenesis, oligodendrocytes, myelination, and astrocytes in the control and LIPUS-treated BCAS groups (n = 1 pooled sample obtained from 4 separate animals per group). **(E)** RT-qPCR analysis of the indicated genes in the control and LIPUS-treated BCAS groups; each gene is plotted relative to the respective control group (n = 18 per group). **(F)** Western blot analysis of GFAP, Olig2, p-eNOS, t-eNOS, CXCR4, and FGF2 on days 3 (n = 10 per group). **(G)** NGF and pro-BDNF plotted against eNOS measured on days 3 and 7 (n = 7–10); the correlation coefficients and *P*-value are indicated. $^{*}P < 0.05$, and $^{**}P < 0.005$ (Student's t-test).

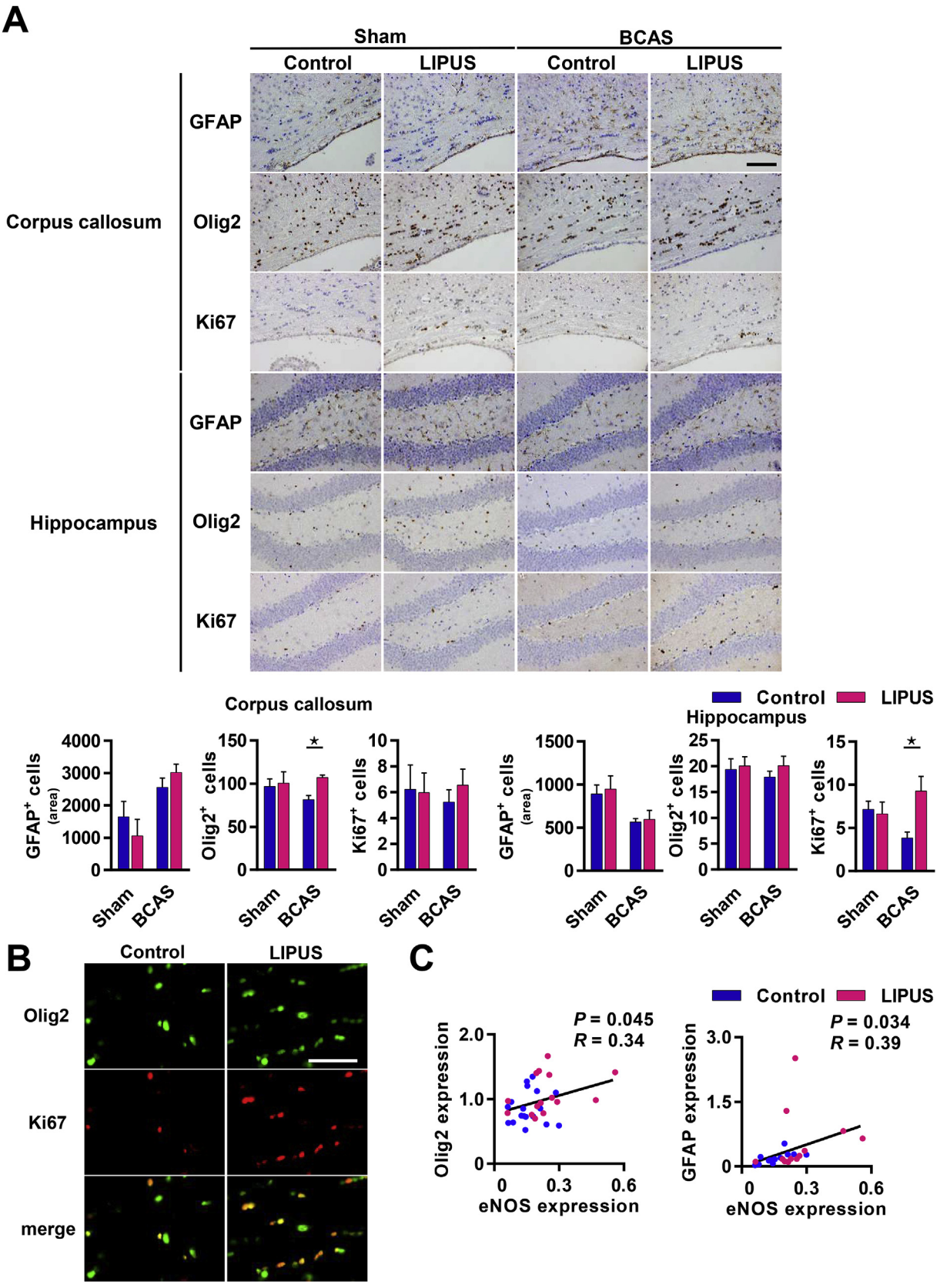

Fig. 4. LIPUS therapy enhances OPC proliferation and activates glia cells associated with eNOS upregulation.
(A) Representative images of corpus callosum and hippocampal sections immunostained for GFAP, Olig2, and Ki67 in control and LIPUS-treated sham mice and in control and LIPUS-treated BCAS mice on day 3. The scale bar represents 100 μm. Quantitative analysis of GFAP-, Olig2-, and Ki67-positive cells in the corpus callosum and hippocampus of mice treated as indicated; n = 3 (sham) and n = 9–10 (BCAS). **(B)** Representative images of corpus callosum section co-immunostained for Olig2 and Ki67 in control and LIPUS-treated mice on day 3. The scale bar indicates 50 μm. **(C)** Olig2 and GFAP mRNA plotted against eNOS mRNA(n = 16 per group); the correlation coefficients and *P*-value are indicated. **P*<0.05 (two-way ANOVA).

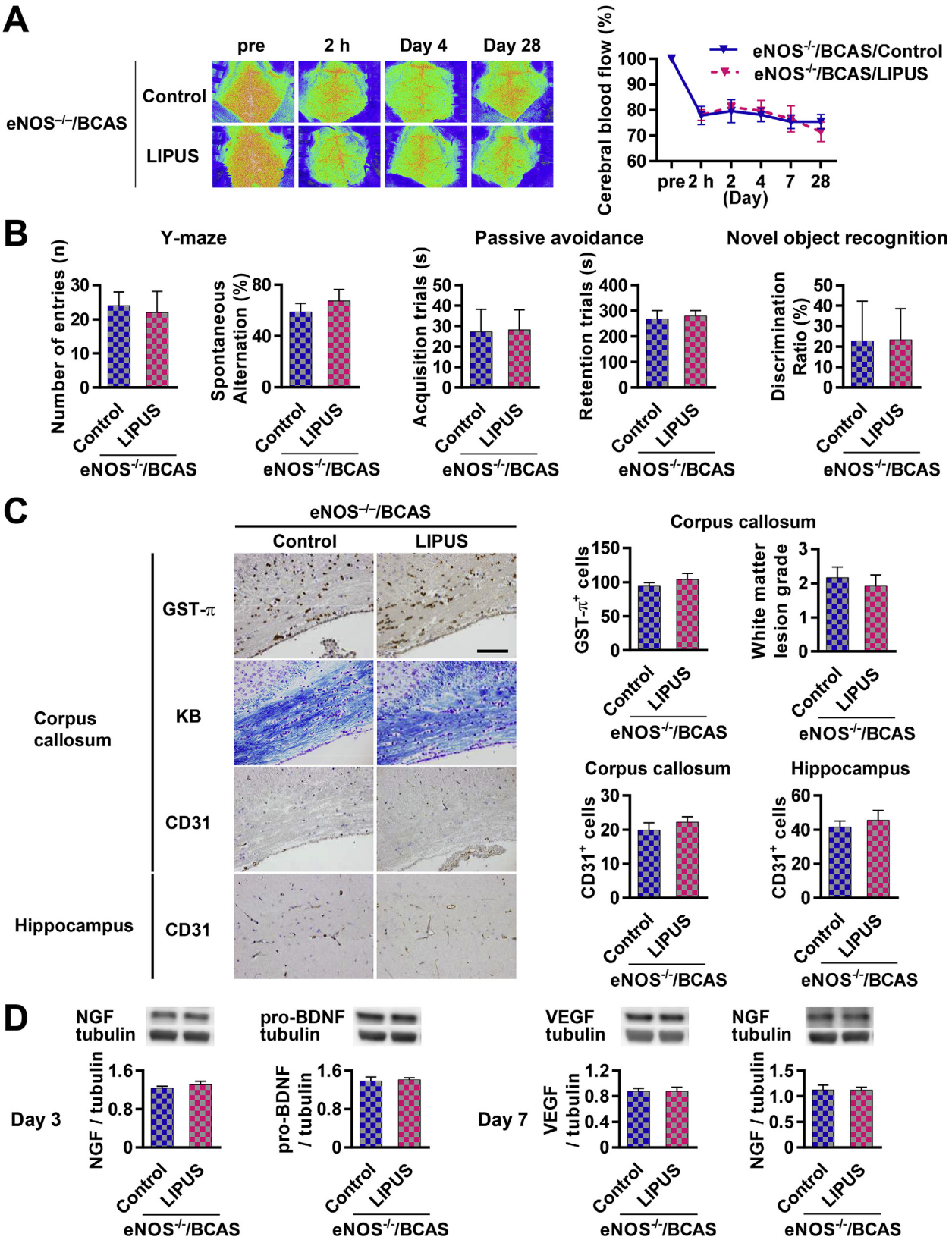

Fig. 5. eNOS is required for the beneficial effects of LIPUS in the VaD model.
(A) Representative laser speckle images showing cerebral blood flow (CBF) measured at the indicated times in control and LIPUS-treated eNOS$^{-/-}$ mice subjected to BCAS surgery. Time-course of CBF in the indicated groups (n = 6 per group). **(B)** Behavioral tests were performed on day 28 in control and LIPUS-treated eNOS$^{-/-}$ mice subjected to BCAS surgery (n = 6 per group). **(C)** Representative images of corpus callosum and hippocampal sections immunostained for GST-π or CD31 or stained with Klüver-Barrera on day 28. The scale bar represents 100 μm. Quantitative analysis of GST-π-positive cells, white matter lesion severity score, and CD31-positive cells in the corpus callosum and hippocampus (n = 6 per group). **(D)** Western blot analysis of NGF, pro-BDNF, and VEGF on day 3 and/or on day 7 (n = 5 per group).

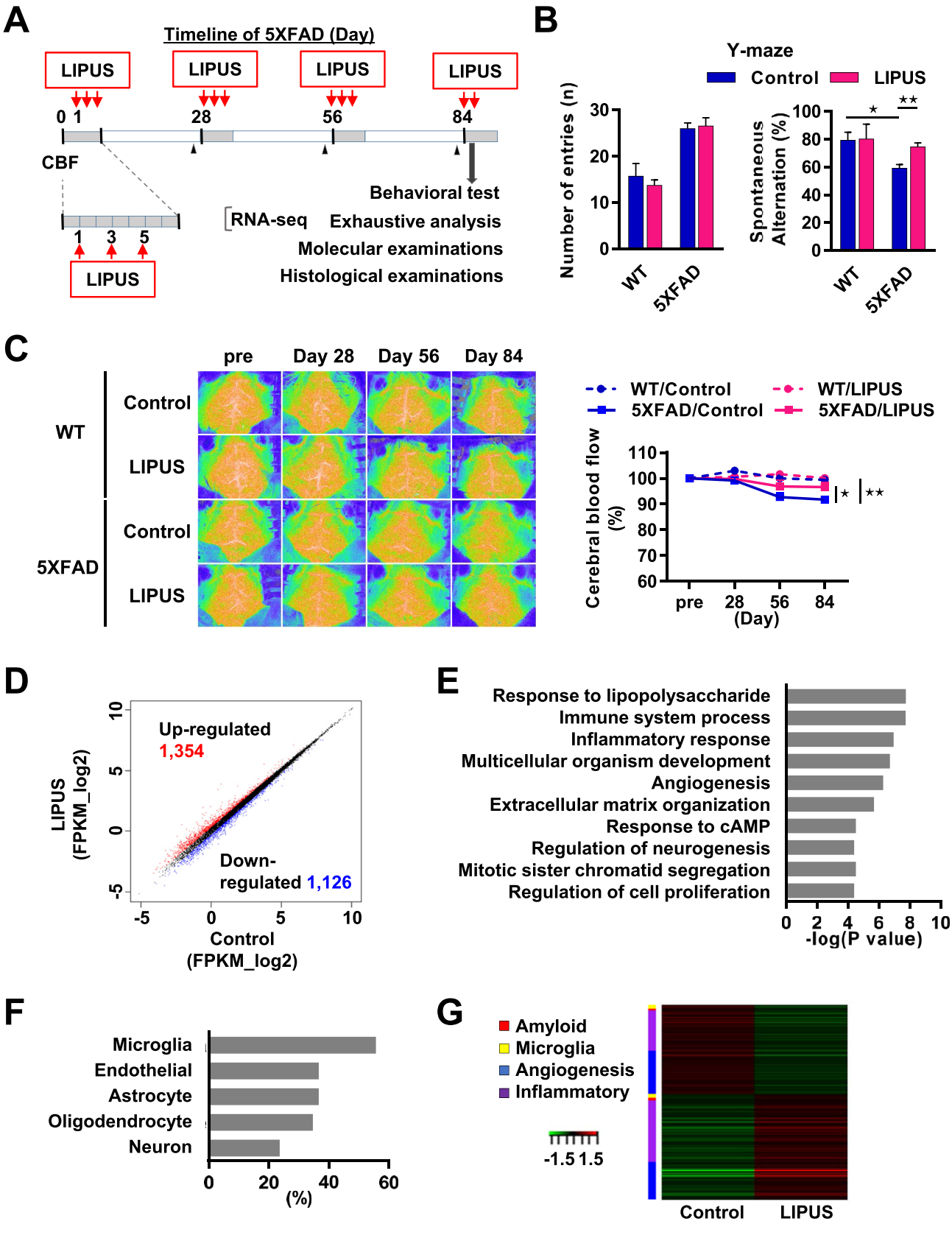

Fig. 6. Whole-brain LIPUS therapy ameliorates cognitive dysfunctions in the AD model.
(A) Timeline of the experiments with 5XFAD mice. **(B)** Summary of Y-maze test results measured on day 86 (n = 18 per group). **(C)** Representative laser speckle images of CBF and the time-course of CBF relative to baseline; n = 3 (WT) and n = 14 (5XFAD). **(D)** Scatter plot depicting differential gene expressions between the LIPUS-treated and control 5XFAD groups, on day 86. Significantly upregulated or downregulated genes are colored in red and blue, respectively. **(E)** Gene ontology (GO) analyses of the significantly upregulated or downregulated genes measured between the LIPUS-treated and control groups. The top ten GO terms are shown in descending order of *P*-value. **(F)** The percentage of differentially regulated genes for each cell type annotated by GO terms. **(G)** Heat map depicting the relative expression of angiogenesis and microglia-related genes in the control and LIPUS-treated groups (n = 1 pooled sample obtained from 4 separate animals per group). $^{*}P<0.05$, $^{**}P<0.005$ and $^{***}P<0.0005$ (two-way ANOVA). LIPUS, low-intensity pulsed ultrasound.

blood pressure in 5XFAD mice (Supplementary Fig. 7A). Moreover, the LIPUS therapy did not cause cramps, paralysis, cerebral hemorrhage, hypothermia, hyperthermia, or death (data not shown) or hyperactivity (Fig. 6B). Importantly, the LIPUS therapy significantly improved cognitive functions in 5XFAD mice in the spontaneous alternation task (Fig. 6B). The LIPUS therapy had no significant effect in the passive avoidance test (Supplementary Fig. 7B). Moreover, consistent with previous finding [17], we found an aging-dependent decrease in CBF in 5XFAD (Fig. 6C). LIPUS had no effect on CBF in wild-type mice for 84 days after the treatment (Fig. 6C). Interestingly, however, this decline in CBF in 5XFAD mice was ameliorated by the LIPUS therapy, resulting in significantly higher CBF in the LIPUS-treated group at 84 days after the treatment (Fig. 6C).

Next, we performed RNA-seq analysis using whole-brain samples to compare the global gene expression patterns between LIPUS-treated and control 5XFAD mice on day 86. We found that nearly 2500 genes were differentially expressed in the LIPUS and the control groups, including 1354 upregulated and 1126 downregulated genes (Fig. 6D). GO term analysis showed that the genes regulated by the LIPUS therapy in the 5XFAD mice encoded key regulators of immune function and angiogenesis (Fig. 6E), similar to the genes identified in the VaD model. We next calculated the number of genes annotated to each type of cells as a percentage of the total number of genes, demonstrating that the majority of genes were annotated to microglia. Interestingly, endothelium-related genes were the second most frequently enhanced genes in this model as well as in the BCAS model (Fig. 6F). The heat map expression confirmed that the LIPUS therapy significantly upregulated and/or downregulated genes related to amyloid, microglia, inflammation, and angiogenesis (Fig. 6G). These results suggest that the LIPUS therapy suppressed chronic inflammatory response of microglias, and that endothelium-related genes were also enhanced in this model.

3.8. LIPUS therapy reduces microgliosis along with eNOS upregulation in the AD model

Based on the results from RNA-seq, we examined microgliosis and angiogenesis in those mice (Fig. 7A). Histological analysis showed a significant reduction in microgliosis in the cortex of 5XFAD mice following the LIPUS therapy, reflecting a decrease in Iba-1-positive cells (Fig. 7A). The number of CD31-positive cells tended to increase in the hippocampus of LIPUS-treated 5XFAD mice compared with the control group (Fig. 7A). Since we found no significant difference between the LIPUS-treated and the control groups, we focused on the 5XFAD group in the subsequent biochemical analyses.

Next, we examined whether the LIPUS therapy affects eNOS expression in the 5XFAD mice since the significance of eNOS as a therapeutic target in AD has been recently reported [4]. Western blot analysis showed that the LIPUS therapy significantly increased t-eNOS protein levels in 5XFAD mice (Fig. 7B), and this increase was correlated with a reduction in Iba-1-positive cells (Fig. 7C). Furthermore, the expression of APP (amyloid precursor protein) and BACE-1 (β-site amyloid precursor protein cleaving enzyme-1), both of which are known to be suppressed by eNOS [18], were significantly decreased by the LIPUS therapy (Supplementary Fig. 7C). Hsp 90 (heat shock protein 90), an activator of eNOS [19], was significantly increased by the LIPUS therapy (Supplementary Fig. 7C). In contrast, the protein levels of both NGF and pro-BDNF were significantly increased in LIPUS-treated mice compared with control mice, whereas VEGF levels were unchanged (Supplementary Fig. 7D). Importantly, we found a positive correlation between eNOS and pro-BDNF as well as in the VaD model (Fig. 7D). Taken together, these results indicate that the whole-brain LIPUS therapy in the AD mice had potential to suppress neuroinflammation through suppression of microglia and amyloid-β (Aβ) accumulation associated with eNOS upregulation.

3.9. LIPUS therapy reduces Aβ plaque in the AD model

Mechanistically, we performed histological and biochemical analyses to examine the effect of the LIPUS therapy on accumulation of Aβ in the brain of 5XFAD mice. Interestingly, we found that LIPUS significantly decreased the Aβ-42 plaque throughout the brain in 5XFAD mice (Fig. 8A). Enzyme-linked immunosorbent assay (ELISA) showed that the amount of Aβ-42 in the triton-soluble fraction (which contains primarily oligomeric Aβ [20]) was decreased in the LIPUS-treated group (Fig. 8B). In contrast, LIPUS had no effect on Aβ-42 levels in the TBS-soluble fraction, which contains primarily monomeric Aβ (Fig. 8B) [20]. Importantly, recruitment of microglia cells to Aβ deposits were enhanced in LIPUS-treated mice compared with control mice (Fig. 8C). These results suggest that the LIPUS therapy enhances the phagocytosis of Aβ plaque.

4. Discussion

In the present study, we report the first experimental evidence that the whole-brain LIPUS therapy markedly improves cognitive dysfunctions without serious side effects in the 2 major mouse models of dementia (VaD and AD) by enhancing the specific cells corresponding to each pathology, and that eNOS plays important roles in mediating the beneficial effects of LIPUS (see Fig. 9). Since large molecules cannot cross the blood-brain barrier [21,22], the strategy to increase the local expression of endogenous neurotrophins is important for dementia. Furthermore, the present study provides 3 important advances in this field. First, our study shows that the whole-brain LIPUS therapy is effective and safe when applied in vivo. Second, we identified the main processes by which LIPUS improves cognitive dysfunctions, namely increased OPC production in the VaD model and reduced microgliosis in the AD model. Third, we were able to demonstrate that eNOS activation plays crucial and common roles in the beneficial effects of LIPUS therapy in both models of dementia.

4.1. LIPUS ameliorates cognitive dysfunctions by promoting OPC-, angiogenesis in the VaD model

The VaD model with BCAS is characterized by WML due to chronic cerebral ischemia, similar to patients with the disorder [23]. OPC proliferation is enhanced in WML in patients with multiple cerebral infarctions, suggesting that white matter has the capacity to regenerate via OPC proliferation following ischemic injury [24]. In the present study, the LIPUS therapy significantly increased the number of both OPCs and oligodendrocytes, suggesting the maturation and differentiation of oligodendrocytes from OPCs, ultimately leading to reduced WML. Moreover, OPCs themselves can contribute to angiogenesis following white matter injury [25]. Thus, LIPUS-induced OPC proliferation and angiogenesis may be a novel strategy that can improve cognitive dysfunction for VaD patients.

4.2. LIPUS ameliorates cognitive dysfunctions by reducing Aβ and microgliosis in the AD model

The primary phenotype in 5XFAD mice includes the progressive accumulation of Aβ and neuroinflammation, thereby mimicking the main pathological features of AD patients [16]. In the present

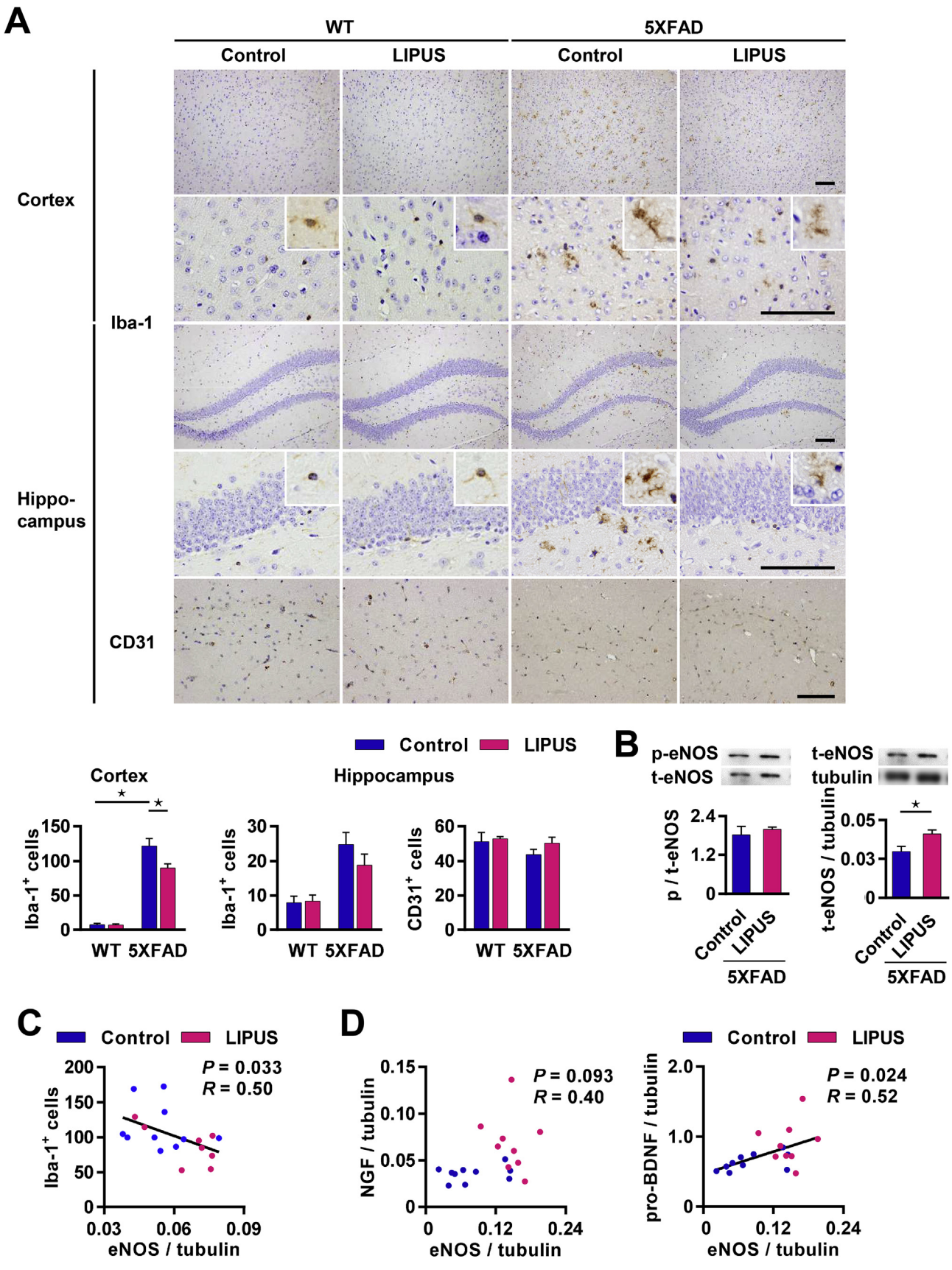

Fig. 7. LIPUS therapy reduces microgliosis in relation to the eNOS expression in the AD model.
(A) Representative images of cortical and hippocampal sections immunostained for Iba-1 (a marker of microglia) and CD31 on day 86. Low-magnification images are shown in the upper panels, and high-magnifications in the lower panels. The scale bars represent 100 μm. Quantitative analysis of Iba-1-positive cells and CD31-positive cells measured in the cortex and/or hippocampus; n = 3 (WT) and n = 11–15 (5XFAD). **(B)** Western blot analysis of p-eNOS and t-eNOS in whole-brain homogenates (n = 9 per group). **(C)** The number of Iba-1-positive cells is plotted against eNOS mRNA level; the correlation coefficient and *P*-value are indicated. The scale bar indicates 50 μm. **(D)** NGF and pro-BDNF plotted against eNOS; the correlation coefficients and *P*-values are indicated. **P*<0.05 (Panel A; two-way ANOVA, B; Student's *t*-test).

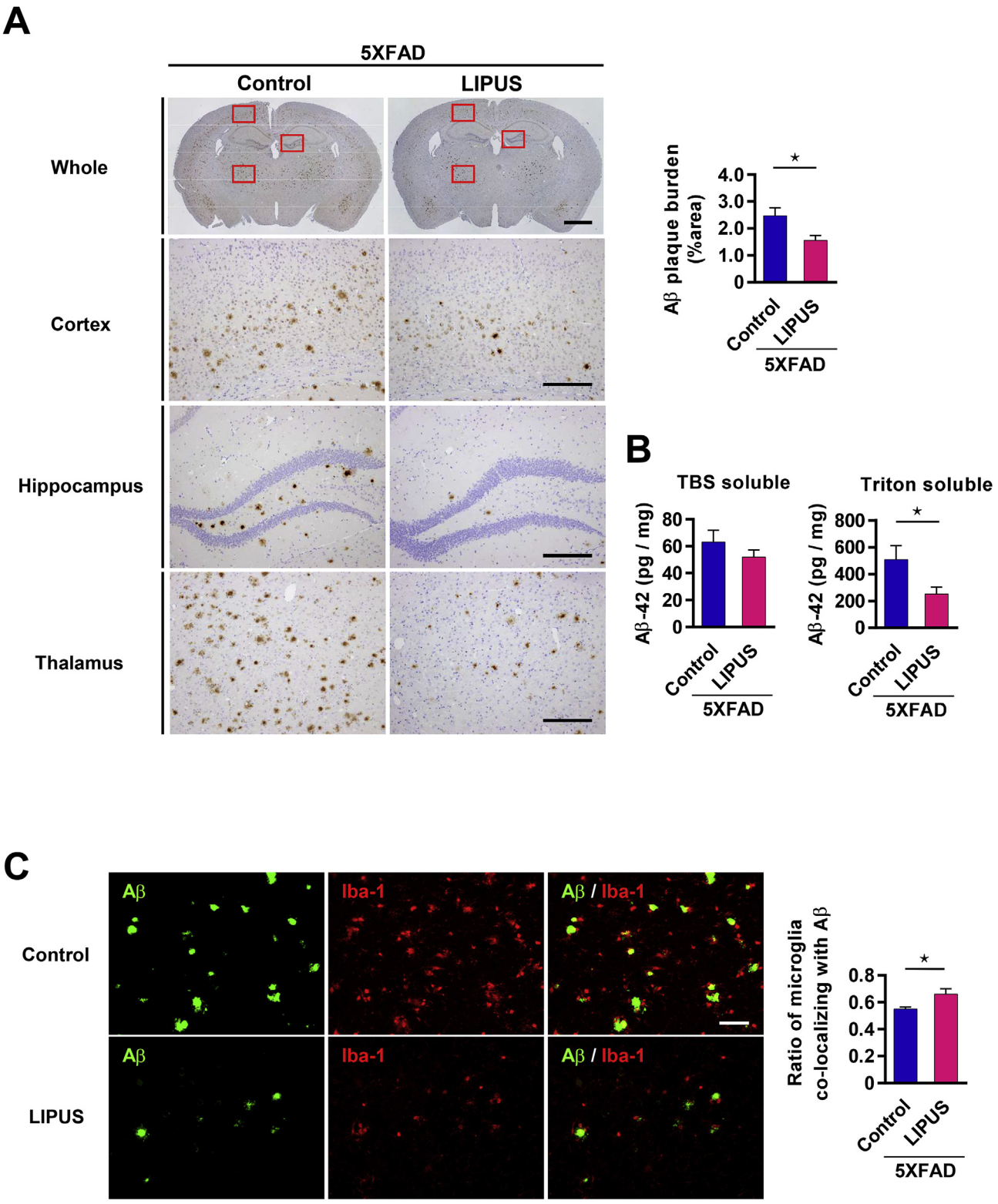

Fig. 8. LIPUS therapy reduces Aβ plaques in the AD model.
(A) Representative images of coronal sections immunostained for Aβ on day 86; the lower images show magnified views of the cerebral cortex, hippocampus, and thalamus. The scale bars represent 500 μm (whole brain) or 50 μm (other rows). Quantitative analysis of Aβ plaques area measured in whole-brain sections (n = 11–15 per group). **(B)** Summary of Aβ-42 measured in whole-brain samples using ELISA (n = 9 per group). **(C)** Representative images of co-immunostaining for Aβ and Iba-1 in control and LIPUS-treated mice on day 86 (n = 6 per group). *P<0.05 (Student's t-test).

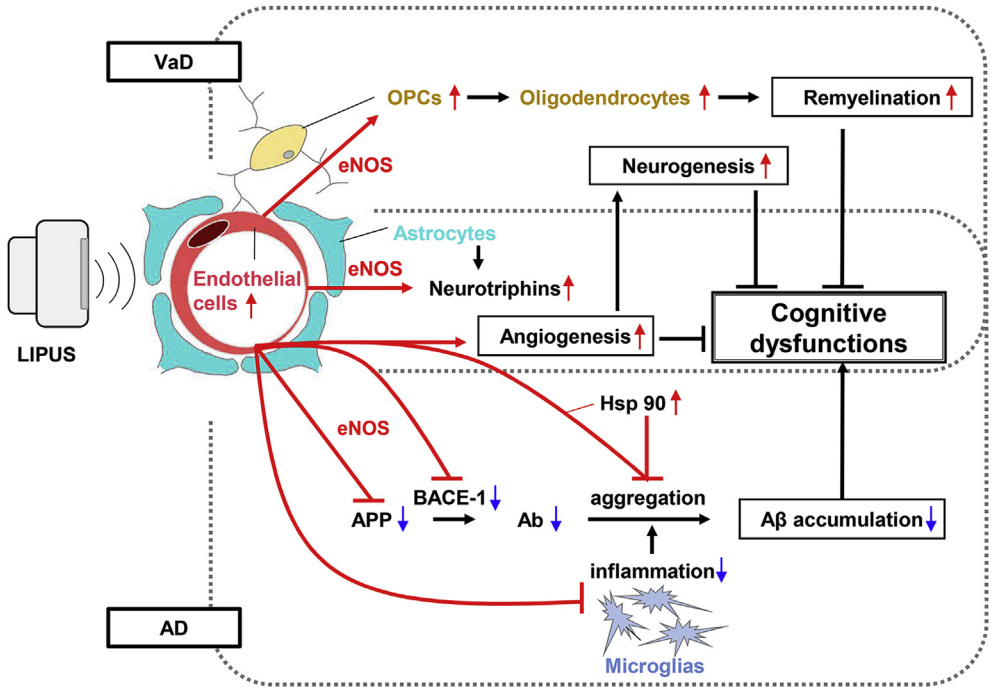

Fig. 9. Schematic diagram showing the proposed mechanisms underlying the beneficial effects of whole-brain LIPUS in the 2 mouse models of dementia.
Whole-brain LIPUS treatment can activate a variety of cell types corresponding to each pathology in the neurovascular unit (i.e., neurons, glial cells, and vascular cells). The present study indicates that activation of endothelial NO synthase (eNOS) is a key component underlying the beneficial effects of the LIPUS therapy in both models of dementia. eNOS increases the proliferation of oligodendrocyte precursor cells (OPCs) in the VaD mouse model and decreases microglias in the AD mouse model. Proliferation of OPCs leads to an increase in mature oligodendrocytes, ultimately leading to re-myelination. Moreover, eNOS may also have significant effects on astrocytes, reported to release neurotrophins. In addition to suppressing microgliosis, eNOS also inhibits the production and accumulation of Aβ. eNOS-induced angiogenesis plays an important role in neurogenesis via a change in cerebral blood flow. Finally, the cognitive dysfunction can be inhibited by re-myelination, angiogenesis, and neurogenesis in the VaD mouse model, and by reduced microgliosis and Aβ plaques, increased angiogenesis in the AD mouse model.

study, the expression of APP and BACE-1 were significantly decreased by the LIPUS therapy, and Aβ was significantly reduced in triton-soluble fraction and histological assessment. Regarding the mechanism of unchanged TBS soluble Aβ levels, Aβ is known to dissolve in a monomer form at concentrations lower than 3 μM, whereas it aggregates at concentrations higher than 3 μM [29]. In the present study, although the total amount of Aβ was actually decreased by LIPUS treatment, more amount of Aβ was produced than the amount that could dissolve in extracellular fluid. Thus, we consider that the amount of Aβ in the extracellular fluid continued to be saturated, resulting in no difference in the TBS soluble fraction. On the other hand, it is generally accepted that microglia-mediated neuroinflammatory responses can promote neurodegeneration in AD [26]. Thus, a strategy to suppress this microglial response could be a therapeutic approach for AD [26,27]. However, since microglia acts in both protective and toxic manners, its function in AD is still controversial. In the present study, the ratio of recruited microglia to phagocytosis for amyloid plaque was significantly higher in the LIPUS-treated group (Fig. 7B). Although the total number of Iba-1-positive microglia decreased by LIPUS, phagocytosis was rather enhanced in the LIPUS-treated group. Besides, Hsp 90, which is known to inhibit aggregation of Aβ [28], was enhanced by LIPUS in the present study, a consistent finding of the previous study [29]. Hsp 90 is promptly recruited by endothelial stimulation of shear stress induced by ultrasonic waves, and enhances eNOS activation [30]. Thus, we consider that LIPUS-induced reduction in Aβ triton fraction and plaque load can be explained, at least in part, by the following mechanisms; (i) reduction in Aβ production, (ii) the changes in characteristics of microglia, and (iii) refolding of Aβ by Hsp 90. Multiple factors may be involved in the mechanisms of LIPUS-induced reduction in Aβ triton fraction and plaque load. Further studies are needed to clarify the mechanisms of Aβ plaque reduction by the LIPUS therapy.

4.3. Important roles of eNOS as a common mechanism in the two mouse models of dementia

Our RNA-seq analyses with 2 different models of dementia revealed that the LIPUS therapy significantly upregulated genes related to vascular endothelial cells. In the VaD model, LIPUS improved CBF promptly after the LIPUS therapy, suggesting that the acute effect of LIPUS on CBF is likely to be mediated by a vasodilating factor rather than angiogenesis. eNOS produces relatively low concentrations of NO, which are essential for maintaining endothelial function and integrity [31,32]. NO exerts a variety of physiological effects, including regulation of vascular tone and angiogenesis [32,33]. Thus, eNOS activation is an effective therapeutic strategy for a variety of cardiovascular diseases [31,32]. Moreover, in the hippocampus, eNOS plays a crucial role in long-term potentiation [34]. In endothelial cells, eNOS localizes in the caveolae, and its activity is controlled by binding with caveolin [30]. Cyclic strain induced by ultrasonic pulse activates mechanotransduction via mechanosensors [35], such as caveolin, leading to eNOS activation [30]. Indeed, in the present study, eNOS was upregulated by LIPUS at both mRNA and protein levels. We also found a significant correlation between eNOS and activated glial cells/molecules in both models; eNOS and Olig2 expression/neurotrophins in the BCAS model and eNOS and Iba-1-positive cells/neurotrophin in the AD model. $eNOS^{-/-}$ mice have activated microglial cells and spontaneously develop cognitive impairment [18]. Moreover, the factors contributing to Aβ reduction, such as microglias, APP, BACE-1, and Hsp 90, are known to be linked with

eNOS [18,30]. Our finding that the beneficial effects of LIPUS are absent in eNOS$^{-/-}$ mice provides further evidence that eNOS plays key roles in mediating the effects of LIPUS.

4.4. Important role of astrocytes in the LIPUS-induced beneficial effects on cognitive functions

Astrocytes play an important role in maintaining neural functions through releasing neurotrophins (e.g. BDNF and NGF), which are increased in response to LIPUS [7, 39]. Since LIPUS-induced increase in neurotrophins was absent in eNOS$^{-/-}$ mice, activation of endothelial cells may have significant effects on astrocytes, resulting in improvement of cognitive functions in the present study. The enhancement of GFAP expression also supports the involvement of astrocytes in the LIPUS-induced beneficial effects on cognitive functions.

4.5. Interpretation of the behavioral improvements

We consider that the behavioral improvements observed in the present study reflect improved cognition. In the present study, Y maze and novel object recognition test were analyzed independently for motor functions because they were corrected by calculating as ratio. In contrast, in passive avoidance test, the improvement of motor performance shortens the latency. In general, BCAS mice show motor dysfunction 3 month after operation [36], while 5XFAD after 9 months of age [37]. In the present study, we performed behavioral tests at 1 month after operation in BCAS mice, and at 6–7 months in 5XFAD mice. In the Y maze test, we found no difference in the number of entries between LIPUS and control groups in both models.

4.6. Study limitations

Several limitations should be mentioned for the present study. First, in the present study, we were unable to examine the contribution of eNOS in 5XFAD mice because this model was technically difficult to generate. Second, the use of 5XFAD mice has some limitations. With this model, we were obviously unable to evaluate tau protein. Furthermore, 5XFAD mouse is a model of forced amyloidosis but not an actual human AD model. Third, we did not use endothelium-specific eNOS$^{-/-}$ mice. However, eNOS is mainly localized in endothelial cells, including the brain, which was also confirmed in the present study. Finally, we did not directly compare the effectiveness between our whole-brain LIPUS therapy and the focused LIPUS therapy to the hippocampus by others [10,11].

5. Conclusions

We were able to demonstrate that the whole-brain LIPUS is an effective and safe therapy for ameliorating cognitive dysfunction induced by either ischemia or overexpression of amyloid-related genes in mice, for which eNOS plays crucial roles to improve cerebral circulatory dysfunction. These findings suggest that whole-brain LIPUS therapy may be beneficial in vascular dementia and AD in humans.

Conflicts of interest

None declared.

Appendix A. Supplementary data

Supplementary data related to this article can be found at https://doi.org/10.1016/j.brs.2018.05.012.

References

[1] Prince AC-H M, Knapp M, Guerchet M, Karagiannidou M. World Alzheimer report 2016. London: Alzheimer's Disease International; 2016. 2016.
[2] Scheltens P, Blennow K, Breteler MM, de Strooper B, Frisoni GB, Salloway S, et al. Alzheimer's disease. Lancet 2016;388:505–17.
[3] O'Brien JT, Thomas A. Vascular dementia. Lancet 2015;386:1698–706.
[4] Katusic ZS, Austin SA. Neurovascular protective function of endothelial nitric oxide- recent advances. Circ J 2016;80:1499–503.
[5] Hanawa K, Ito K, Aizawa K, Shindo T, Nishimiya K, Hasebe Y, et al. Low-intensity pulsed ultrasound induces angiogenesis and ameliorates left ventricular dysfunction in a porcine model of chronic myocardial ischemia. PLoS One 2014;9:e104863.
[6] Shindo T, Ito K, Ogata T, Hatanaka K, Kurosawa R, Eguchi K, et al. Low-intensity pulsed ultrasound enhances angiogenesis and ameliorates left ventricular dysfunction in a mouse model of acute myocardial infarction. Arterioscler Thromb Vasc Biol 2016;36:1220–9.
[7] Liu SH, Lai YL, Chen BL, Yang FY. Ultrasound enhances the expression of brain-derived neurotrophic factor in astrocyte through activation of TrkB-Akt and Calcium-CaMK signaling pathways. Cerebr Cortex 2017;27:3152–60.
[8] Zhao L, Feng Y, Hu H, Shi A, Zhang L, Wan M. Low-intensity pulsed ultrasound enhances nerve growth factor-induced neurite outgrowth through mechanotransduction-mediated ERK1/2-CREB-Trx-1 signaling. Ultrasound Med Biol 2016;42:2914–25.
[9] Chang CJ, Hsu SH, Lin FT, Chang H, Chang CS. Low-intensity-ultrasound-accelerated nerve regeneration using cell-seeded poly(D,L-lactic acid-co-glycolic acid) conduits: an in vivo and in vitro study. J Biomed Mater Res B Appl Biomater 2005;75:99–107.
[10] Lin WT, Chen RC, Lu WW, Liu SH, Yang FY. Protective effects of low-intensity pulsed ultrasound on aluminum-induced cerebral damage in Alzheimer's disease rat model. Sci Rep 2015;5:9671.
[11] Huang SL, Chang CW, Lee YH, Yang FY. Protective effect of low-intensity pulsed ultrasound on memory impairment and brain damage in a rat model of vascular dementia. Radiology 2017;282:113–22.
[12] Salcedo R, Oppenheim JJ. Role of chemokines in angiogenesis: CXCL12/SDF-1 and CXCR4 interaction, a key regulator of endothelial cell responses. Microcirculation 2003;10:359–70.
[13] Shing Y, Folkman J, Sullivan R, Butterfield C, Murray J, Klagsbrun M. Heparin affinity: purification of a tumor-derived capillary endothelial cell growth factor. Science 1984;223:1296–9.
[14] McKinnon RD, Matsui T, Dubois-Dalcq M, Aaronson SA. FGF modulates the PDGF-driven pathway of oligodendrocyte development. Neuron 1990;5:603–14.
[15] Patel JR, McCandless EE, Dorsey D, Klein RS. CXCR4 promotes differentiation of oligodendrocyte progenitors and remyelination. Proc Natl Acad Sci U S A 2010;107:11062–7.
[16] Oakley H, Cole SL, Logan S, Maus E, Shao P, Craft J, et al. Intraneuronal beta-amyloid aggregates, neurodegeneration, and neuron loss in transgenic mice with five familial Alzheimer's disease mutations: potential factors in amyloid plaque formation. J Neurosci 2006;26:10129–40.
[17] Wiesmann M, Zerbi V, Jansen D, Lutjohann D, Veltien A, Heerschap A, et al. Hypertension, cerebrovascular impairment, and cognitive decline in aged AbetaPP/PS1 mice. Theranostics 2017;7:1277–89.
[18] Katusic ZS, Austin SA. Endothelial nitric oxide: protector of a healthy mind. Eur Heart J 2014;35:888–94.
[19] Garcia-Cardena G, Fan R, Shah V, Sorrentino R, Cirino G, Papapetropoulos A, et al. Dynamic activation of endothelial nitric oxide synthase by Hsp90. Nature 1998;392:821–4.
[20] Hao W, Liu Y, Liu S, Walter S, Grimm MO, Kiliaan AJ, et al. Myeloid differentiation factor 88-deficient bone marrow cells improve Alzheimer's disease-related symptoms and pathology. Brain 2011;134:278–92.
[21] Pardridge WM. Drug and gene delivery to the brain: the vascular route. Neuron 2002;36:555–8.
[22] Patel MM, Patel BM. Crossing the blood-brain barrier: recent advances in drug delivery to the brain. CNS Drugs 2017;31:109–33.
[23] Shibata M, Ohtani R, Ihara M, Tomimoto H. White matter lesions and glial activation in a novel mouse model of chronic cerebral hypoperfusion. Stroke 2004;35:2598–603.
[24] Miyamoto N, Tanaka R, Shimura H, Watanabe T, Mori H, Onodera M, et al. Phosphodiesterase III inhibition promotes differentiation and survival of oligodendrocyte progenitors and enhances regeneration of ischemic white matter lesions in the adult mammalian brain. J Cerebr Blood Flow Metabol 2010;30:299–310.
[25] Pham LD, Hayakawa K, Seo JH, Nguyen MN, Som AT, Lee BJ, et al. Crosstalk between oligodendrocytes and cerebral endothelium contributes to vascular remodeling after white matter injury. Glia 2012;60:875–81.
[26] Block ML, Zecca L, Hong JS. Microglia-mediated neurotoxicity: uncovering the molecular mechanisms. Nat Rev Neurosci 2007;8:57–69.
[27] Zenaro E, Pietronigro E, Della Bianca V, Piacentino G, Marongiu L, Budui S, et al. Neutrophils promote Alzheimer's disease-like pathology and cognitive decline via LFA-1 integrin. Nat Med 2015;21:880–6.
[28] Evans CG, Wisen S, Gestwicki JE. Heat shock proteins 70 and 90 inhibit early stages of amyloid beta-(1-42) aggregation in vitro. J Biol Chem 2006;281:33182–91.

[29] Miyasaka M, Nakata H, Hao J, Kim YK, Kasugai S, Kuroda S. Low-intensity pulsed ultrasound stimulation enhances Heat-shock protein 90 and mineralized nodule formation in mouse calvaria-derived osteoblasts. Tissue Eng 2015;21:2829–39.
[30] Bredt DS. Nitric oxide signaling specificity–the heart of the problem. J Cell Sci 2003;116:9–15.
[31] Vanhoutte PM, Zhao Y, Xu A, Leung SW. Thirty years of saying NO: sources, fate, actions, and misfortunes of the endothelium-derived vasodilator mediator. Circ Res 2016;119:375–96.
[32] Shimokawa H. 2014 Williams Harvey Lecture: importance of coronary vasomotion abnormalities-from bench to bedside. Eur Heart J 2014;35:3180–93.
[33] Albrecht EW, Stegeman CA, Heeringa P, Henning RH, van Goor H. Protective role of endothelial nitric oxide synthase. J Pathol 2003;199:8–17.
[34] Kantor DB, Lanzrein M, Stary SJ, Sandoval GM, Smith WB, Sullivan BM, et al. A role for endothelial NO synthase in LTP revealed by adenovirus-mediated inhibition and rescue. Science 1996;274:1744–8.
[35] McCormick SM, Saini V, Yazicioglu Y, Demou ZN, Royston TJ. Interdependence of pulsed ultrasound and shear stress effects on cell morphology and gene expression. Ann Biomed Eng 2006;34:436–45.
[36] Nishio K, Ihara M, Yamasaki N, Kalaria RN, Maki T, Fujita Y, et al. A mouse model characterizing features of vascular dementia with hippocampal atrophy. Stroke 2010;41:1278–84.
[37] Jawhar S, Trawicka A, Jenneckens C, Bayer TA, Wirths O. Motor deficits, neuron loss, and reduced anxiety coinciding with axonal degeneration and intraneuronal Abeta aggregation in the 5XFAD mouse model of Alzheimer's disease. Neurobiol Aging 2012;33. 196.e129-140.